Available online at www.sciencedirect.com
SCIENCE DIRECT
Solid State Communications 138 (2006) 279–284
solid state communications
www.elsevier.com/locate/ssc

Interplay between the local structural disorder and the length of structural coherence in stabilizing the cubic phase in nanocrystalline ZrO_2

Milen Gateshki [a], Valeri Petkov [a,*], Taeghwan Hyeon [b], Jin Joo [b], Markus Niederberger [c], Yang Ren [d]

[a] *Department of Physics, Central Michigan University, Mt Pleasant, MI 48859, USA*
[b] *National Creative Research Initiative Center for Oxide Nanocrystalline Materials and School of Chemical and Biological Engineering, Seoul National University, Seoul 151-744, South Korea*
[c] *Max–Planck Institute of Colloids and Interfaces, Potsdam D-14424, Germany*
[d] *Advanced Photon Source, Argonne National Laboratory, Argonne, IL 60439, USA*

Received 11 November 2005; received in revised form 5 March 2006; accepted 10 March 2006 by J.W.P. Hsu
Available online 29 March 2006

Abstract

The atomic-scale structure of three nanocrystalline ZrO_2 samples obtained by different techniques and possessing a different length of structural coherence has been studied using high-energy X-ray diffraction and the atomic pair distribution function technique. The studies reveal that all samples show a monoclinic-like local atomic ordering. Only when the length of structural coherence exceeds 1 nm the atomic arrangement evolves into a cubic-type one. The result underlines the importance of both the local structural disorder and the length of structural coherence, i.e. the spatial extent of longer-range atomic order, in stabilizing the technologically important cubic zirconia at room temperature.

PACS: 61.10.Nz; 81.07.Bc

Keywords: A. Nanocrystalline materials; C. X-ray diffraction; C. Structure determination

Zirconia has attracted lasting interest due to its useful properties finding applications in fuel cells, catalysts and advanced ceramics [1]. At room temperature crystalline ZrO_2 adopts a monoclinic-type structure. Most applications of ZrO_2, however, are based on its cubic polymorph which is stable at high temperatures (>2640 K) only. This has prompted extensive research on finding an efficient way to stabilize the technologically important cubic phase of crystalline ZrO_2 at room temperature. It has been found that a stabilization could be achieved by doping bulk zirconia with a small amount of Y, Ca or Hf [2]. The doping does stabilize the cubic phase of zirconia at room temperature but impairs some of material's properties [3]. Recently, the attention has shifted to producing zirconia powders with a cubic-like structure at room temperature just by reducing the crystallite size to a few nanometers. This novel technology approach is advantageous since doping the material, and the associated deterioration of some material's properties, are both avoided. In a recent paper [4], we reported that nanosize ZrO_2 crystals produced by ball milling adopt a cubic-like structure on average but locally their atomic arrangement is indeed monoclinic-like. The finding revealed that the presence of a mismatch between the local and longer-range atomic arrangement is a factor playing a key role in stabilizing the technologically important cubic phase of zirconia at room temperature. To verify this conclusion we studied two more zirconia samples obtained by different, yet nanotechnology-based, preparation routes and summarize our results in this brief paper.

One of the samples (hereafter referred as sample **1**) was synthesized by hydroxide precipitation of zirconyl chloride. The first step in this reaction route was followed by redispersion in aqueous medium using sonification and employing nitric acid as a peptizing agent. Analytical ultracentrifugation showed a particular narrow nanoparticle size distribution ranging from 1.5 to 3.5 nm with a maximum at 2.5 nm [5]. The other sample (hereafter referred as sample **2**) was obtained by a non-hydrolytic sol–gel reaction between zirconium (IV) isopropoxide and zirconium (IV) chloride at 610 K. This reaction route allows to synthesize multigram quantities of nanocrystalline

* Corresponding author. Tel.: +1 989 774 3395.
E-mail address: petkov@phy.cmich.edu (V. Petkov).

0038-1098/$ - see front matter © 2006 Elsevier Ltd. All rights reserved.
doi:10.1016/j.ssc.2006.03.013

zirconia consisting of particles with a size in the range of 3–4 nm as TEM studies show (Fig. 1 in Ref. [6]). Details of the preparation route may be found in the original paper [6]. We studied these two samples, together with the previously characterized ball-milled zirconia showing a nanoparticle size distribution ranging from 250 to 400 nm (hereafter referred as sample **3**), and crystalline monoclinic ZrO_2 powder with a particle size distribution in the range of 1–10 μm (purchased from Cerac; hereafter referred as sample **4**). The samples showed quite different degrees of structural perfection as demonstrated by the very different full widths at half maxima (FWHM) of the Bragg peaks in the corresponding X-ray diffraction (XRD) patters presented in Fig. 1. The diffraction patterns were collected at the 11-ID-C beamline (Advanced Photon Source, Argonne National Laboratory) using synchrotron radiation with wavelength of 0.1076 Å. X-rays of higher energy were used to obtain diffraction data to higher values of the wave vector, Q, which is important for the success of the atomic pair distribution function (PDF) analysis employed by us. The measurements were carried out in symmetric transmission geometry and scattered radiation was collected with an intrinsic germanium detector connected to a multichannel analyzer. Several runs were conducted with each of the samples and the resulting XRD patterns averaged out to improve the statistical accuracy of the diffraction data. As can be seen in Fig. 1 the XRD pattern of bulk monoclinic zirconia (sample **4**) shows well defined Bragg peaks to wave vectors as high as 10 $Å^{-1}$, as might be expected for a material that is a perfect

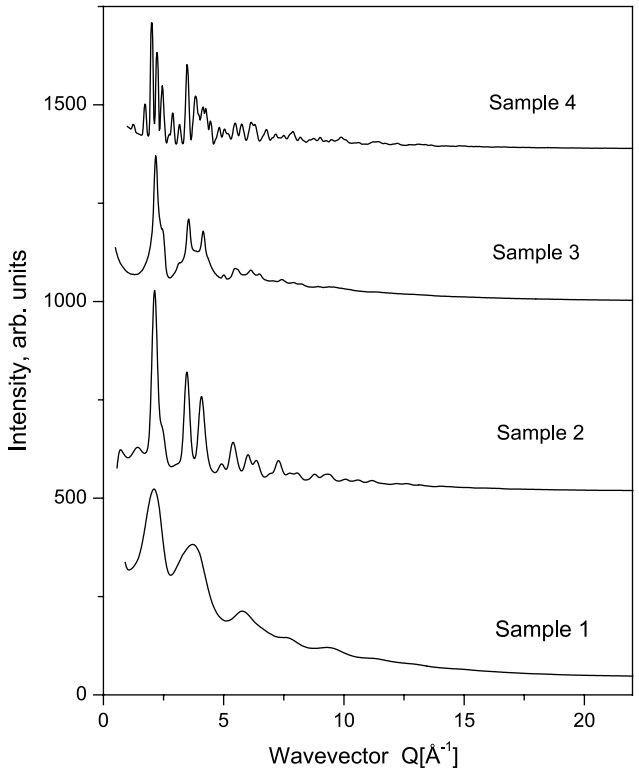

Fig. 1. Experimental X-ray diffraction patterns of crystalline monoclinic zirconia (sample **4**) and three nanocrystalline samples labeled as described in the text.

crystalline solid. The Bragg peaks in the diffraction patterns of nanocrystalline samples **2** and **3** are rather broad and merge into an oscillating diffuse component already at Q-values as low as 5–7 $Å^{-1}$. Sample **1** shows only three very broad Bragg-like features at low wave vectors. The size of coherently scattering domains, L, in each of the samples was estimated from the FWHM of the first Bragg-like peak/feature in the corresponding diffraction patterns using the Scherrer equation

$$L = \frac{k\lambda}{\mathrm{FWHM}\cos(\Theta)} \tag{1}$$

where λ is the wavelength of the radiation used, Θ is the Bragg angle and k is a constant ($\sim$0.94). That size was found to be approx. 2–4 nm and $\sim$0.1 μm for samples **1**–**4**, respectively. When this result is compared to the previous TEM estimates [4–6] one may conclude that samples **1** and **2** are most likely single-domain nanoparticles while the particles in samples **3** and **4** are very likely to be divided into several domains that are misoriented with respect to each other.

Diffraction patterns like those exhibited by samples **1**–**3** are typical for materials with limited structural coherence and are difficult to be analyzed by traditional techniques for structure determination. However, when reduced to the corresponding atomic PDFs, they become a structure-sensitive quantity lending itself to structure determination. The atomic pair distribution function, $G(r)$, is defined as follows

$$G(r) = 4\pi r[\rho(r) - \rho_0] \tag{2}$$

where $\rho(r)$ and ρ_0 are the local and average atomic number densities, respectively, and r is the radial distance. It peaks at characteristic distances separating pairs of atoms and thus reflects the atomic-scale structure. The PDF $G(r)$ is the Fourier transform of the coherent part of the experimentally observable XRD pattern, called a total structure function, $S(Q)$, i.e.

$$G(r) = (2/\pi)\int_{Q=o}^{Q_{\max}} Q[S(Q) - 1]\sin(Qr)\mathrm{d}Q \tag{3}$$

where Q is the magnitude of the wave vector ($Q = 4\pi \sin\theta/\lambda$). As can be seen from Eqs. (2) and (3), the PDF is another representation of the powder XRD data. However, exploring the diffraction data in real space is advantageous, especially in the case of materials of limited structural perfection. First, the total scattering, including Bragg scattering as well as diffuse scattering, contributes to the PDF. In this way both the average, longer-range atomic structure, manifested in the Bragg-like peaks, and the structural distortions of any type, manifested in the diffuse component of the diffraction pattern, are reflected in the PDF. And second, the atomic PDFs do not imply any periodicity and can be used to study the atomic ordering in materials showing any degree of structural perfection, ranging from crystals [7] to glasses [8]. Recently, the atomic PDF approach has been successfully applied to nanocrystalline materials as well [7,9]. The experimental XRD patterns of Fig. 1 were subject to appropriate corrections and converted to

the corresponding atomic PDFs, shown in Fig. 2, using the program RAD [10].

As can be seen in Fig. 2, the experimental PDF for crystalline monoclinic ZrO_2 is rich in well-defined structural features extending to very high real-space distances, as it should be with a material possessing long-range atomic order. The PDFs for the nanocrystalline sample are also rich in well defined features but those vanish already at approximately 10, 20 and 25 Å for samples **1**–**3**, respectively. Obviously, these samples have an atomic arrangement very well defined at nanoscale distances but lack the extended order of usual bulk crystals. Furthermore, the atomic PDFs for the nanocrystalline samples decay to zero at interatomic distances that are shorter than the average nanoparticle size as obtained by TEM experiments [4–6]. On top of that, the atomic PDFs for samples **1**–**3** decay to zero at interatomic distances that are even somewhat shorter than the size of coherently scattering domains obtained from the FWHM of the Bragg peaks in the corresponding diffraction patterns (see the estimates above). This observation suggests that the three nanocrystalline samples studied in this work are very likely to exhibit local structural distortions that further reduce their structural coherence. And it is this disorder and not the size of the nanocrystallites that is the factor limiting the longer-range order in those materials. Such local structural distortions are frequently observed with nanostructured materials and are ascribed to surface relaxation effects [11], and/or to the presence of extended structural defects [12]. The structural distortions are more pronounced with sample **1** since its PDF decays to zero faster than those of the other two nanocrystalline zirconia samples (**2** and **3**) do. The first peak in the experimental PDFs shown in Fig. 2 (see the inset) is positioned at approx. 2.13(2) Å. Such an average Zr–O distance is characteristic for crystalline monoclinic ZrO_2. For reference, this distance is at about 2.28 Å with crystalline cubic ZrO_2 at 1673 K [13] and at about 2.23 Å with cubic ZrO_2 stabilized at room temperature by doping with 18 mol% of $YO_{1.5}$ [14]. This observation shows that all three nanocrystalline samples studied by us have almost the same immediate Zr–O atomic coordination, resembling that occurring in monoclinic ZrO_2. The second PDF peak, corresponding to the first Zr–Zr distances, appears at about 3.45 Å for samples **1**, **3** and **4**, and at about 3.60 Å for sample **2**. A Zr–Zr distance of 3.45 Å is typical for monoclinic ZrO_2, while a distance of 3.60 Å agrees with that observed with cubic and tetragonal ZrO_2 [13,14]. Thus the results of the preliminary studies of the experimental PDFs suggest that the three nanocrystalline samples share almost the same immediate atomic ordering (i.e. a first coordination shell), resembling that of monoclinic ZrO_2. Differences in the atomic ordering in the different samples start appearing at second neighbor and longer-range interatomic distances.

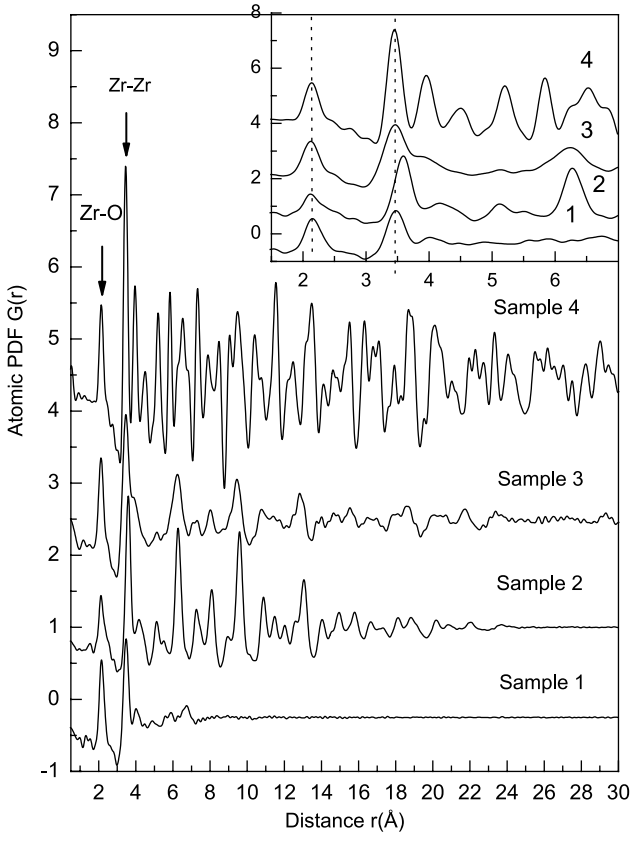

Fig. 2. Experimental PDFs for crystalline monoclicnic zirconia (sample **4**) and three nanocrystalline samples (**1**–**3**). The first two peaks in the experimental PDFs are marked with the corresponding atomic pairs. The lower part of the experimental data is given on an enlarged scale in the inset. As can be seen, the first Zr–O distance appears at about 2.13 Å for all for samples. The first neighbor Zr–Zr distance in sample **2** differs from that exhibited by the other samples. The broken lines in the inset are a guide for the eye.

To reveal the fine details in the structure of the studied nanomaterials we compared the corresponding experimental PDFs with calculated ones based on several structural models. The approach of using a structure-sensitive experimental quantity, such as the atomic PDF, to discriminate between competing models is widely applied in crystallography. Here we apply it, as it has been done before [4,7,9,12], to find a realistic model for nanocrystalline materials with an imperfect yet well-defined atomic-scale structure. The degree of agreement between the model and experimental data was assessed by computing a goodness-of-fit factor, R_{wp}

$$R_{wp} = \left\{ \frac{\sum w_i (G_i^{exp.} - G_i^{calc.})^2}{\sum w_i (G_i^{exp.})^2} \right\}^{1/2}, \quad (4)$$

where $G^{exp.}$ and $G^{calc.}$ are the experimental and calculated PDFs, respectively, and w_i are weighting factors reflecting the statistical quality of the individual data points.

The atomic PDF for crystalline zirconia (sample **4**) was approximated with a model based on the well-known structure data for bulk monoclinic ZrO_2. A fragment of the structure of monoclinic ZrO_2 crystal is given in Fig. 3(a). The fit yielded structural parameters that are both in good agreement with previous results [4] and reproduce the experimental data very well, as can be seen in Fig. 4. The agreement well documents the fact that the atomic PDF provides a reliable quantitative basis for structure determination.

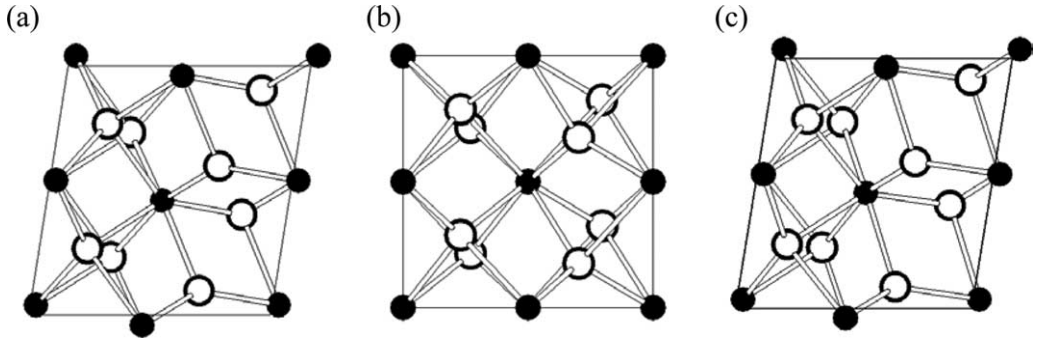

Fig. 3. Fragments from the crystal structure of bulk monoclinic ZrO_2 (a), a structure featuring a cubic unit cell and local monoclinic-type ordering (b) and a distorted monoclinic ZrO_2-type structure (c). A model PDF calculated on the basis of fragment (a) approximates very well the experimental PDF for bulk zirconia (sample **4**); a model calculated on the basis of fragment (b) approximates very well the structure of nanocrystalline samples **2** and **3**; a model calculated on the basis of fragment (c)—that of nanocrystalline sample **1**.

The corresponding value of R_{wp} is ~22%. It may be noted that the goodness-of-fit factor achieved with the PDF-based structural modeling appears somewhat high when compared to R_{wp} factors usually resulted from Rietveld refinement of diffraction data in reciprocal space. This does not indicate an inferior structure determination (Table 1 in Ref. [4]) but merely reflects the fact that, the atomic PDF differs from the corresponding XRD pattern and is a quantity much more sensitive to local ordering in materials. As a result, R_{wp}'s greater than 15% are common with PDF refinements even of well crystallized materials [4,9]. The inherently higher absolute value of the goodness-of-fit factors resulted from PDF-based refinements does not affect their functional purpose as a quantity allowing to differentiate between competing structural models.

Next we approached ball-milled nanocrystaline zirconia (sample **3**) with an atomic arrangement based on the unit cell of cubic zirconia whereas the local symmetry of the atoms within the cell conformed to that of the monoclinic space group $P2_1/c$. The reasons for adopting this approach are described in our previous study [4] in full detail. That model reproduces the corresponding experimental PDF data very well as can be seen in Fig. 4. The corresponding R_{wp} is as good as one may expect with PDF-based studies. The structural parameters of the model are reported in Table 2 in Ref. [4]. The model describes nanocrystalline zirconia obtained by ball milling as a material having a longer-range structure (showing at interatomic distances >10 Å) of a cubic type and a local atomic ordering (showing at interatomic distances <10 Å) resembling that of bulk monoclinic ZrO_2 crystal.

The three-dimensional structure of sample **2** was approached with three models based on the three crystalline polymorphs of ZrO_2: the cubic one occurring at temperatures higher than 2640 K, the tetragonal one occurring in the temperature range from 1440 to 2640 K and the monoclinic one occurring at room temperature. It should be mentioned that bulk cubic and tetragonal-ZrO_2 are very similar to each other from a structural point of view and cannot be easily distinguished when the material is in a nanocrystalline state. That is why, and based on the discussion in the paper of Joo et al. [6], we concentrated on tetragonal-type models with an orthogonal unit cell very similar to that found with cubic zirconia and on monoclinic-type (non-orthogonal unit cell) structure models. Besides, structure models based on cubic zirconia are incompatible with the first neighbor Zr–O distances observed in the samples studied in the present work (Fig. 2). Two tetragonal-type models were constructed—one with isotropic and the other—with highly anisotropic mean square atomic displacements. The first one did not match the experimental data well and was unambiguously ruled out. The

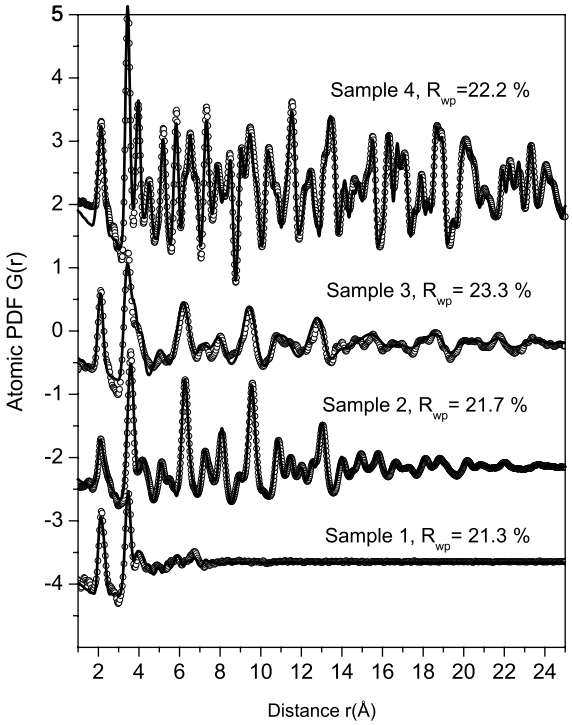

Fig. 4. Experimental (symbols) and model (full line) PDFs for bulk monoclinic crystalline ZrO_2 (sample **4**) and three nanocrystalline samples (**1**–**3**). The experimental PDF for monoclinic ZrO_2 is approximated very well with a model (Fig. 3(a)) based on crystal structure data from literature sources [15]. The experimental PDFs for samples **2** and **3** (ball-milled) are well approximated with a model based on a cubic unit cell and local monoclinic-like order (Fig. 3(b)). The experimental PDF for sample **1** is well approximated with a model based on a distorted ZrO_2-type monoclinic structure (Fig. 3(c)). The corresponding goodness-of-fit factors, R_{wp}, are shown for each of the models.

second one matched the experimental PDF better and confirmed the findings of our preliminary studies that sample **2** too, just like nanocrystalline materials **1** and **3**, exhibits considerable local structural distortions leading to a displacement of the atoms off their positions in the ideal crystal lattice. A model based on the monoclinic-type structure of zirconia also showed some promise but failed to reproduce the observed Zr–Zr distance of 3.60 Å. The failure of the models based on the crystalline modifications of ZrO_2 prompted us to explore a hybrid model featuring an average structure of cubic symmetry (i.e. an average structure that may be described in terms of a cubic unit cell) and local atomic ordering of a monoclinic type. This model turned out to be quite successful in describing the atomic arrangement in nanocrystalline zirconia obtained by ball milling (sample **3** [4]). Such a model was constructed, refined against the experimental PDF data for sample **2** and reproduced it very well as can be seen in Fig. 4 and demonstrated by the corresponding R_{wp} factor. A fragment of the model is represented in Fig. 3(b). The refined values of the structural parameters of that model (unit cell constant, atomic positions and root-mean square atomic displacements of the atomic species in sample **2**) are listed in Table 1.

Finally, we turned our attention to sample **1** showing a very limited length of structural coherence, i.e. a very high degree of local structural disorder. Models based on orthogonal unit cells (cubic, tetragonal and the hybrid one described above) failed in reproducing the experimental data. The only model that was able to reproduce not only the strong PDF peaks showing up below 4 Å but also the less pronounced PDF features between 4 and 10 Å was based on a considerably distorted, monoclinic ZrO_2-type structure. A fragment of the model atomic configuration is presented in Fig. 3(c). That model reproduced the experimental PDF data for sample **1** very well as can be seen in Fig. 4. The refined values of the corresponding structural parameters are presented in Table 2.

In summary, the atomic arrangement in three nanocrystalline zirconia samples obtained by different synthetic routes and possessing different lengths of structural coherence has been studied by synchrotron radiation scattering experiments and the atomic PDF technique. Although the structural coherence length in these nanostructured materials is reduced to 1–2.5 nm only, their three-dimensional structure still may be described in the usual crystallographic terms of a repetitive unit cell containing only a few atoms. A common feature in the three nanocrystalline samples studied is the monoclinic-like-type of the immediate atomic ordering (that showing up below 10 Å).

Only when the nanomaterials are ordered at longer-range distances (samples **2** and **3**) the type of the atomic ordering evolves into a higher symmetry one that is better described in terms of a repetitive, orthogonal unit cell of the cubic type occurring in bulk crystalline ZrO_2. It appears that not only the presence of a mismatch between the local and longer-range atomic ordering but also the length of structural coherence (i.e. the spatial extent of the longer-range order) plays an important role in stabilizing the technologically important cubic zirconia at room temperature. Only nanocrystalline zirconia samples that are locally less ordered than at longer range distances and exhibit a structural coherence length of at least 2 nm evolve into materials with an average cubic-type structure. This suggests a new approach to producing cubic-type zirconia that is stable at room temperature. It could be achieved by tuning up the particular nanotechnological routes and/or by a careful annealing of the initially highly disordered samples until a material with the pure stoichiometry of ZrO_2, the desired length of structural coherence, a cubic-type longer-range atomic order and respective macroscopic properties is obtained.

Table 1
Structure data for nanocrystalline zirconia, sample **2**

Atomic coordinates/ thermal factors	x	y	z	U_{iso} (Å^2)
Zr	1/4	0	1/4	0.012(1)
O1	0.05(1)	0.30(2)	0.43(1)	0.075(1)
O2	0.481(2)	0.745(1)	0.463(1)	0.004(1)

The unit cell is cubic with $a=5.107(1)$ Å and the atomic positions conform to the monoclinic $P2_1/c$ space group. The fractional coordinates of the Zr atoms where not refined.

Table 2
Structure data for nanocrystalline zirconia, sample **1**

Unit cell constants and angles	a (Å)	b (Å)	c (Å)	β (°)
	4.974(3)	5.335(4)	5.384(2)	99.20(1)
Atomic coordinates/ thermal factors	x	y	z	U_{iso} (Å^2)
Zr	0.277(1)	0.044(1)	0.213(2)	0.008(1)
O1	0.088(1)	0.347(1)	0.337(1)	0.030(1)
O2	0.425(1)	0.730(1)	0.494(1)	0.027(1)

The unit cell and the atomic positions within it conform to the monoclinic $P2_1/c$ space group.

Acknowledgements

Thanks are due to M. Beno from APS, Argonne National Laboratory for the help with the synchrotron experiments. The work was supported by NSF through grant DMR 0304391(NIRT). The Advanced Photon Source is supported by DOE under contract W-31-109-Eng-38.

References

[1] E.C. Subbarao, Ferroelectrics 102 (1990) 267.
[2] C.J. Howard, R.J. Hill, B.E. Reichert, Acta Crystallogr, B 44 (1988) 116.
[3] V.F. Petrunin, V.V. Popov, Z. Hongzhi, A.A. Timofeev, Inorg. Mater. 40 (2004) 251.
[4] M. Gateshki, V. Petkov, S.K. Pradhan, G. Williams, Y. Ren, Phys. Rev. B 71 (2005) 224107.
[5] A.S. Deshpande, N. Pinna, P. Beato, M. Antonietti, M. Niederberger, Chem. Mater. 16 (2004) 2599.

[6] J. Joo, T. Yu, Y.W. Kim, H.M. Park, F. Wu, J.Z. Zhang, T. Hyeon, J. Am. Chem. Soc. 125 (2003) 6553.
[7] (a) B.H. Toby, T. Egami, Acta Crystallogr, A 48 (1992) 336;
(b) V. Petkov, I.-K. Jeong, J.S. Chung, M.F. Thorpe, S. Kycia, S.J.L. Billinge, Phys. Rev. Lett. 83 (1999) 4089.
[8] V. Petkov, S.J.L. Billinge, S.D. Sashtri, B. Himmel, Phys. Rev. Lett. 85 (2000) 3436.
[9] S.J.L. Billinge, M.G. Kanatzidis, Chem. Commun. 7 (2004) 749.
[10] V. Petkov, J. Appl. Cryst. 22 (1989) 387.
[11] B. Gilbert, F. Huang, H.Z. Zhang, G.A. Waychunas, G.F. Banfield, Science 305 (2004) 65.
[12] V. Petkov, Y. Peng, G. Williams, B. Huang, D. Tomalia, Y. Ren, Phys. Rev. B 72 (2005) 195402.
[13] D.K. Smith, C.F. Cline, J. Am. Ceram. Soc. 45 (1962) 249.
[14] M. Yashima, S. Sasaki, M. Kakihana, Y. Yamaguchi, H. Arashi, M. Yoshimura, Acta Crystallogr, B 50 (1994) 663.
[15] R.E. Hann, P.R. Suitch, J.L. Pentecost, J. Am. Ceram. Soc. 68 (1985) 285.